

$^{208}\text{Pb}(^3\text{He}, ^3\text{He}') \text{ Reaction at } 43.7 \text{ MeV}^*$ 

F. Todd Baker† and Robert Tickle

*Cyclotron Laboratory, Department of Physics, The University of Michigan, Ann Arbor, Michigan 48105*

(Received 10 November 1971)

Angular distributions for the ( $^3\text{He}, ^3\text{He}'$ ) reaction exciting the first  $2^+$ ,  $3^-$ ,  $4^+$ , and  $5^-$  levels of  $^{208}\text{Pb}$  have been measured from  $13$  to  $50^\circ$  using a bombarding energy of  $43.67 \text{ MeV}$ . The data were analyzed using both a collective model and a microscopic model. The microscopic calculations used the wave functions of Gillet, Green, and Sanderson. The distorted-wave Born-approximation calculations do not provide good fits at very forward angles; this problem appears to become more severe with increasing multipolarity. As Park and Satchler have recently pointed out, the interference between the Coulomb and nuclear parts of the form factor allows one to measure the phase of the effective microscopic interaction. The results of the present experiment indicate that this phase is near  $\pi/3$  for the  $^{208}\text{Pb}(^3\text{He}, ^3\text{He}')$  reaction.

## I. INTRODUCTION

Inelastic scattering is usually analyzed in terms of the collective model or the microscopic model. The collective-model interaction is obtained by deforming the optical potential which fits the elastic scattering. For deuterons, tritons, and helions ( $^3\text{He}$ ), the imaginary parts of the optical potentials extend to much larger radii than the real parts; as a consequence the inelastic cross section for these light composite particles as computed by the collective model is almost wholly due to the *imaginary* part of the interaction. A microscopic description of inelastic scattering, on the other hand, assumes an effective interaction which is *real* and is often obtained by folding a nucleon-nucleon interaction into the density distribution of the projectile.

Recently Park and Satchler<sup>1,2</sup> have drawn attention to this inconsistency and have suggested that the phase of the effective nuclear interaction used in microscopic calculations can be determined by measuring the interference between it and the real Coulomb interaction.

In the present work angular distributions for the ( $^3\text{He}, ^3\text{He}'$ ) reaction exciting the first  $2^+$ ,  $3^-$ ,  $4^+$ , and  $5^-$  levels of  $^{208}\text{Pb}$  have been carefully measured between  $13$  and  $50^\circ$  where the interference effects of Coulomb excitation (CE) are expected to be most pronounced. Where possible, the data are analyzed to obtain the phase of the effective interaction.

## II. EXPERIMENTAL PROCEDURE

Helions accelerated to  $43.67 \text{ MeV}$  by the University of Michigan 83-in. cyclotron<sup>3</sup> were focused on a  $1.5\text{-mg/cm}^2$   $^{208}\text{Pb}$  target enriched to 98%. The inelastically scattered particles were detected by an array of position-sensitive detectors

placed on the image surface of the first of the three spectrographs which comprise the magnetic-analysis system. Background was minimized by removing all slits from the scattering chamber. The angular convergence of the beam was  $0.8^\circ$  and the angular acceptance of the analyzing system was  $1.0^\circ$  for scattering angles smaller than  $32^\circ$ , and  $2.0^\circ$  for larger angles; the scattering angle was therefore known to  $\pm 0.9^\circ$  in the regions of maximum Coulomb-nuclear interference. Day-to-day normalization of data was done by measurement of the elastic peak at  $25^\circ$ . Experimental errors shown in the figures include both statistical errors and the uncertainty of background subtraction.

## III. ANALYSIS

## A. Collective Model

All analysis was performed using the University of Michigan version of DWUCK<sup>4</sup> which has been modified<sup>5</sup> to include a Gaussian microscopic interaction. The collective-model analysis was performed in the standard way by identifying the interaction as the first term of a Taylor-series expansion of the optical potential. The optical parameters of Parkinson *et al.*,<sup>6</sup> shown in Table I, have been used throughout. CE has been included in the form suggested by Bassel *et al.*<sup>7</sup> using a radius parameter of  $1.4 \text{ F}$ . The view that the meaningful parameter is the deformation length  $\beta_L R \equiv \delta_L$ , rather than the deformation parameter  $\beta_L$ , has been adopted; thus the collective calculations assume equal values of  $\delta_L$  for the real, imaginary, and Coulomb interactions.

It should be pointed out that, due to the strong effects of CE for this reaction, the extraction of spectroscopic information from distorted-wave calculations is somewhat unreliable. For example

the effect of varying the Coulomb radius in the form factor for the  $L=3$  transition was examined; changing the radius parameter from 1.4 to 1.2 F resulted in a 20% change in the extracted value of  $\delta_3^2$ .

### B. Microscopic Model

The effective nucleon-helion interaction suggested by Park and Satchler<sup>1,2</sup> has been used:

$$v(r) = -(22.5 \pm 2.5) \exp[-(0.2 \text{ F}^{-2})r^2] \text{ MeV}. \quad (1)$$

The upper sign is for neutrons and the lower for protons.

The particle-hole wave functions of Gillet, Green, and Sanderson (GGs)<sup>8</sup> were used. The full wave functions for the  $3^-$  (45 components) and  $2^+$  (4 components) states were used; for the  $5^-$  and  $4^+$  levels only components having amplitudes  $|(x+y)| \geq 0.1$  were included. The single-particle energies listed by GGS<sup>8</sup> were used with the exception of those for the  $3p_{3/2}$ ,  $2f_{5/2}$ , and  $3p_{1/2}$  proton levels; more-recent experimental evidence indicates that these energies should be near 0.65, 0.94, and 0.13 MeV, respectively. The bound-state wave functions were calculated using the parameters listed in Table I and by adjusting the well depths to reproduce the assumed binding energies; well depths near 60 MeV for protons and near 47 MeV for neutrons were found for all levels. The bound-state parameters for protons were determined by Batty and Greenlees<sup>9</sup>; these parameters correctly predict the binding energies and the charge distribution for  $^{208}\text{Pb}$ . The neutron bound-state parameters are those suggested by Park and Satchler<sup>1</sup>; these lead to reasonable spectroscopic factors for neutron-transfer experiments and are therefore expected to be correct in the tail regions which are most important for the strongly absorbed helions.

The radial form factors,  $F_L^{jj'}$ , were calculated for each component of each wave function:

$$F_L^{jj'}(r_h) = \int u_{n'l'j'}(r) u_{n_l j}(r) g_L(r, r_h) r^2 dr. \quad (2)$$

The  $u$ 's are the radial wave functions and  $g_L$  is the  $L$ -pole moment of the interaction of Eq. (1). The unprimed (primed) quantum numbers refer to the particle (hole) wave functions. The radial

form factors were then weighted with the appropriate reduced matrix elements<sup>10</sup>  $\langle lj || T_{LSJ} || l'j' \rangle$  (only  $S=0$  contributions were considered) and the wave-function amplitudes  $(x+y)_{jj'}$  to obtain the form factor,  $F_L(r_h)$ , for each transition.

Distorted-wave calculations were performed using complex form factors  $F_L(r_h)e^{i\alpha}$ ; in each case  $\alpha=0$  corresponds to an attractive, real potential.

### C. Choice of $R_{\text{max}}$ and $l_{\text{max}}$

The form factor for CE extends to large radii; for this reason distorted-wave Born-approximation (DWBA) calculations must be performed to large radii and must include many partial waves if this effect is to be properly included. The present calculations used 102 partial waves. The effects of varying  $l_{\text{max}}$  and  $R_{\text{max}}$  were investigated for each transition.

For the  $L=4, 5$  transitions 102 partial waves appeared to be completely adequate for the angular range where the data were obtained. No change in predicted angular distributions was observed when  $R_{\text{max}}$  was increased from 40 to 50 F, and so  $R_{\text{max}}=50$  F was judged to be adequate and was used for all  $L=4, 5$  calculations where CE was included.

The  $L=3$  calculation appears to have converged for  $l_{\text{max}}=101$  for the angular range where data were obtained. Noticeable, but essentially insignificant changes in the predicted angular distributions were observed as  $R_{\text{max}}$  was increased from 40 to 60 F. Increasing  $R_{\text{max}}$  further resulted in no change in the predicted angular distributions, so  $R_{\text{max}}=60$  F was used for all  $L=3$  calculations where CE was included.

Predicted angular distributions for the  $L=2$  transition show significant changes for angles smaller than  $25^\circ$  as  $R_{\text{max}}$  is increased from 40 F. An  $R_{\text{max}}$  of 80 F appears still to be too small, but was used for all  $L=2$  calculations. From the  $l_{\text{max}}$  dependence of the calculations for angles greater than  $25^\circ$ , 102 partial waves seem to be adequate; for smaller angles the calculations appear to be nearly converged and additional partial waves would probably not significantly alter the DWBA predictions. It is interesting to note that

TABLE I. Optical potentials and bound-state parameters.

	$V$ (MeV)	$r_0$ (F)	$a$ (F)	$W$ (MeV)	$r_0'$ (F)	$a'$ (F)	$r_{0c}$ (F)	$\lambda$
Distorted waves	175	1.14	0.723	17.5	1.6	0.901	1.4	
Collective form factors	175	1.14	0.723	17.5	1.6	0.901	1.4	
Neutron bound state		1.23	0.65					26.5
Proton bound state		1.28	0.76				1.2	18.0

if  $R_{\max}$  is chosen to be too small, e.g., 50 F, which one might guess from the semiclassical guide

$$R_{\max} \approx (l_{\max} + 2\eta)/k,$$

the approximate  $l_{\max}$  convergence of the calculations is not obtained for  $l_{\max} = 101$ . All  $L=2$  calculations are probably accurate for angles greater than  $25^\circ$  and are probably within 30% of the "true" DWBA predictions for smaller angles. All calculations where CE was not included used  $l_{\max} = 35$  and  $R_{\max} = 40$  F.

#### IV. EXPERIMENTAL RESULTS

##### A. Collective Model

The results of the collective calculations with and without CE are shown in Fig. 1. Inclusion of CE improves the quality of the fits for the  $L=2, 3,$  and  $4$  transitions and worsens the fit for the  $L=5$  transition. There is an obvious problem in fitting the small-angle data; this error evidently increases with increasing multipolarity.

The spectroscopic parameters,  $\delta_L$  and  $B(L)$ , obtained from the collective-model analysis are listed in Table II. The reduced transition rates,  $B(L)$ , are in Weisskopf single-particle units and are defined as

$$B(L) = \frac{Z^2 (3+L)^2}{4\pi (2L+1)} \left( \frac{\delta_L}{1.2A^{1/3}} \right)^2. \quad (3)$$

Also listed are the  $B(EL)$  values determined by Ziegler and Peterson<sup>11</sup> using the  $^{208}\text{Pb}(e, e')$  reaction and the  $B(L)$  values determined by Saudinos *et al.*<sup>12</sup> using the  $^{208}\text{Pb}(p, p')$  reaction. The  $B(L)$  determined by the present experiment are in poor agreement with the  $B(EL)$  of Ziegler and Peterson; the agreement with the  $(p, p')$  results, however, is quite good with the exception of  $B(5)$ .

##### B. Microscopic Model

For the microscopic-model calculations CE was included using the collective model; the values of  $\delta_L$  determined by the collective analysis were used in these calculations.

Figure 2 shows distorted-wave calculations for the  $L=3$  transition using  $\alpha=0$  (real, attractive),

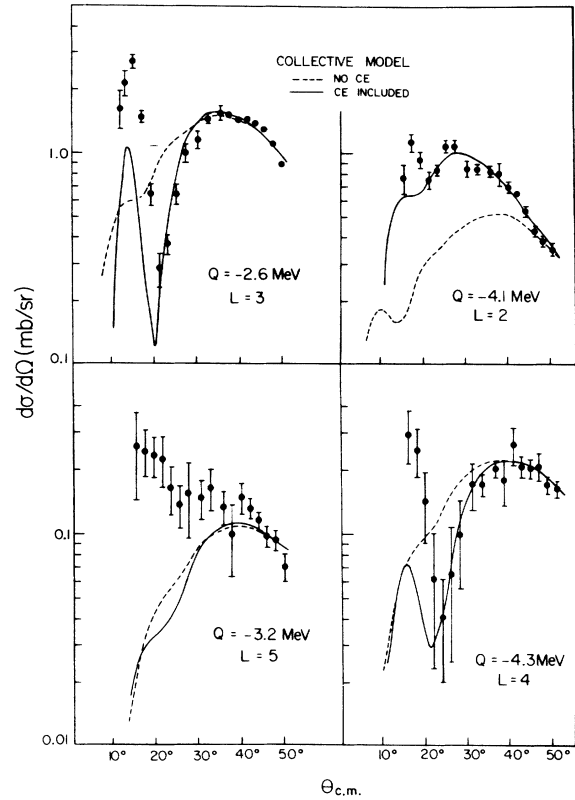


FIG. 1. DWBA calculations for the reaction  $^{208}\text{Pb}-(^3\text{He}, ^3\text{He}')$  assuming a collective model with equal deformation lengths  $\delta_L$ . The extracted  $\delta_L$  are listed in Table II.

$\alpha = \pi/2$  (imaginary, attractive), and  $\alpha = \pi/3$  (complex, attractive). The  $\alpha = \pi/3$  calculation fits the experimental data quite well although the cross section at angles smaller than  $20^\circ$  is still underestimated.

The distorted-wave calculations for all four transitions are shown in Fig. 3; a form-factor phase of  $\pi/3$  was used for all calculations. Again, as for the collective calculations, only the  $L=5$  transition is more poorly fitted after the inclusion of CE. Although the results from the microscopic calculations are still considerably smaller than the experimental data for  $L \geq 3$  at small angles, an appreciable improvement over the collective

TABLE II. Summary of spectroscopic results and comparison with the results of other experiments.

Q (MeV)	L	$\delta_L$ (F)	$B(L)$ (s.p.u.) (this exp.)	$B(EL)$ (s.p.u.)	$B(L)$ (s.p.u.)	$V_L$ (dimensionless)
				( $e, e'$ ) Reference 13	( $p, p'$ ) Reference 14	
-2.6	3	0.59	19.2	39.5	19.5	2.2
-3.2	5	0.24	3.5	14.0	8.1	1.7
-4.1	2	0.30	4.9	8.1	6.4	3.2
-4.3	4	0.30	5.2	26.0	4.6	5.3

calculations is evident.

The magnitudes of the predicted cross sections shown in Fig. 3 were, in fact, smaller than the data; the curves were adjusted by assuming an isoscalar enhancement,  $V_L$ , of the effective interaction of Eq. (1). The required enhancements are listed in Table II. If one accepts the effective interaction as being reasonable and the bound-state wave functions as being approximately correct, the  $V_L$ 's may be interpreted as being indicative of the adequacy of the particle-hole wave functions ( $V_L = 1$  implies a "correct" wave function). The present experiment verifies the already well-known fact that shell-model calculations are more successful for the negative-parity states than for the positive-parity states of  $^{208}\text{Pb}$ ; i.e., larger isoscalar enhancements are required for the  $L = 2, 4$  transitions than for the  $L = 3, 5$  transitions. The enhancements for the transitions to the  $3^-$  and  $5^-$  states are approximately what would be expected in light of GGS<sup>8</sup> calculated  $B(EL)$  values. The enhancement for the  $2^+$  level is somewhat smaller than might have been expected; the calculated<sup>8</sup>  $B(E2)$  was  $\approx 20$  times smaller than experiment; whereas  $(V_2)^2$  is only  $\approx 10$ . The  $B(E2)$

calculation, however, neglected the important ( $g_{9/2}, i_{13/2}^{-1}$ ) neutron configuration. The large value of  $V_4$  indicates a gross inadequacy of the  $4^+$  wave function.

It should be emphasized that  $V_L$  is only an approximate indication of the quality of each wave function. The main reason is the uncertainty of the neutron bound-state parameters, a subject which has been fully discussed by Park and Satchler.<sup>1</sup> Also, exchange effects have not been included in the present calculation; although these effects are not well understood for helions, Park and Satchler<sup>1</sup> have investigated the use of a pseudo-potential to include exchange effects and find appreciable (factors of 2 or 3) changes in the magnitudes of the predicted cross sections.

## V. DISCUSSION

### A. Transition Rates

The  $B(L)$  extracted in the present experiment were all considerably smaller than the  $B(EL)$  values from ( $e, e'$ ) experiments which measure the "true" electromagnetic transition rates. As pointed out in Sec. III, the  $B(L)$  are uncertain, but it

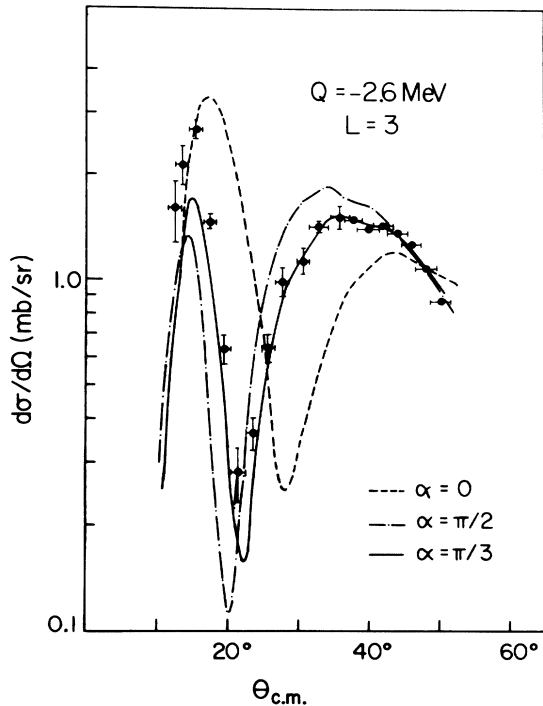


FIG. 2. DWBA calculations for the reaction  $^{208}\text{Pb}-(^3\text{He}, ^3\text{He}')$  for excitation of the 2.615-MeV  $3^-$  level of  $^{208}\text{Pb}$  assuming a microscopic model. The normalizations are arbitrary to facilitate comparison of the three calculations. The phase of the effective interaction,  $\alpha$ , is defined in the text.

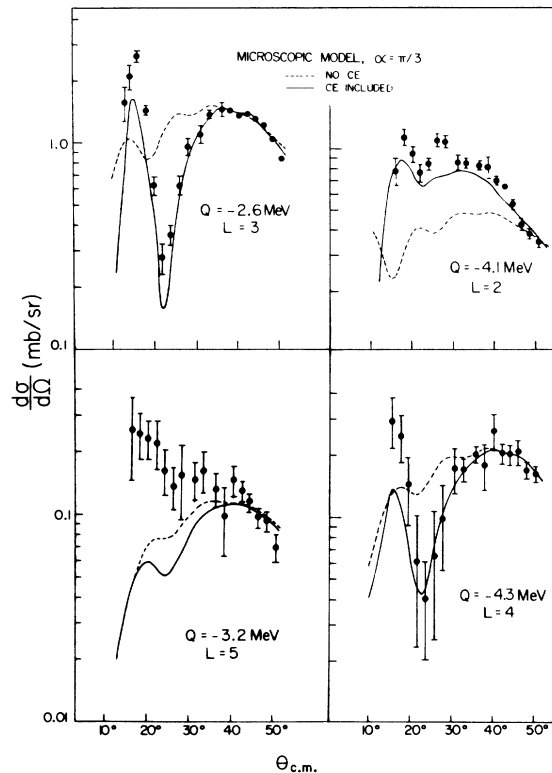


FIG. 3. DWBA calculations for the reaction  $^{208}\text{Pb}-(^3\text{He}, ^3\text{He}')$  assuming a microscopic model. The required isoscalar enhancements,  $V_L$ , are listed in Table II.

is felt that no reasonable change in the analysis would bring the  $B(L)$  into agreement with the  $B(EL)$ . The most probable reason for this disagreement is that, as pointed out by Bernstein<sup>13</sup> for  $(\alpha, \alpha')$  reactions, one does not expect equality of these transition rates except in cases where the excited state may be described as a mass vibration. Strictly speaking, this is true only for  $T=0$  projectiles, such as  $\alpha$  particles, which interact equally strongly with protons and neutrons in the target; one expects, however, that similar, although more complicated, arguments for helions would lead to an expected inequality of transition rates to states poorly described as mass vibrations. Thus, for example, it is not surprising to find  $B(5) \neq B(E5)$  for the 3.2-MeV  $5^-$  level, since this state is well known<sup>14</sup> to be dominated by the  $(g_{9/2}, p_{1/2}^{-1})$  neutron configuration.

#### B. Phase of the Effective Interaction

The phase  $\alpha$  of the microscopic interaction of Eq. (1) was determined to be near  $\pi/3$ . This value is somewhat smaller than might have been expected when compared with the collective-model form factor, which is more imaginary (i.e.,  $\alpha$  is closer to  $\pi/2$ ). The improved fits for all transitions, however, would seem to indicate that perhaps the microscopic model is to be preferred, and that the collective calculations provide only an approximate guide to the phase of the interaction.

*Note added in proof:* It should be noted that the assumption has been made that the real and imaginary parts of the microscopic interaction have identical shapes. This may not be physically accurate, and the phase of the transition amplitude will certainly depend on the relative shapes of the real and imaginary parts of the form factor.

#### C. Relative Strength of Coulomb Excitation

As pointed out in Sec. V A, one does not necessarily expect agreement between the  $B(EL)$  determined by inelastic electron scattering and the  $B(L)$  measured by the  $({}^3\text{He}, {}^3\text{He}')$  reaction. The as-

sumption that the CE deformation length is equal to the nuclear  $\delta_L$  is therefore suspect and could be responsible for the poor fits at forward angles for the  $L=4, 5$  transitions. One would expect the CE  $\delta_L$  to imply a reduced transition rate  $B(L)$  equal to  $B(EL)$ . To investigate this possibility the microscopic calculations for the  $L=3, 4, 5$  transitions were repeated using CE strengths equivalent to  $B(EL)$  values of 37, 20.5, and 15.8 single-particle units (s.p.u.), respectively. It was found, again using  $\alpha = \pi/3$ , that the fits obtained were in fact worse. Thus the problem at small angles remains. Furthermore, these calculations raise the additional question of why the CE transition rates are not consistent with previously measured  $B(EL)$  values.

#### VI. SUMMARY

From a study of angular distributions for the  ${}^{208}\text{Pb}({}^3\text{He}, {}^3\text{He}')$  reaction, we conclude that the microscopic model yields its best results when the effective interaction is complex. Our analysis shows, for the specific cases considered, the phase angle is approximately  $\pi/3$ .

Since the Coulomb interaction extends to great distances, one must, when including CE, be especially careful to use a sufficient number of partial waves and to compute the radial integrals to large radii. 102 partial waves and  $R_{\text{max}} = 60$  F seemed adequate for  $L=3, 4, 5$ . For  $L=2$  at small angles our analysis indicates that  $R_{\text{max}}$  should be greater than 80 F and that more than 102 partial waves are required.

Best fits to the experimental data, especially at small angles, were obtained for the lowest multipoles. As the multipolarity increased, the fits were worse and, for the  $L=5$  angular distribution, omission of CE improved the fit.

#### ACKNOWLEDGMENTS

We are grateful to G. R. Satchler, both for arousing our interest in this problem and for several enlightening communications.

\*Work supported in part by the U. S. Atomic Energy Commission.

†Present address: Department of Physics, Rutgers University, New Brunswick, New Jersey 08903.

<sup>1</sup>J. Y. Park and G. R. Satchler, *Particles Nuclei* **1**, 233 (1971).

<sup>2</sup>G. R. Satchler, *Phys. Letters* **33B**, 385 (1970); and private communication.

<sup>3</sup>W. C. Parkinson, R. S. Tickle, P. T. J. Bruinsma, J. Bardwick, and R. Lambert, *Nucl. Instr. Methods* **18**,

**19**, 92 (1962).

<sup>4</sup>P. D. Kunz, unpublished.

<sup>5</sup>F. T. Baker and R. Tickle, to be published.

<sup>6</sup>W. C. Parkinson, D. L. Hendrie, H. H. Duhm, J. Mahoney, J. Saudinos, and G. R. Satchler, *Phys. Rev.* **178**, 1976 (1969).

<sup>7</sup>R. H. Bassel, G. R. Satchler, R. M. Drisko, and E. Rost, *Phys. Rev.* **128**, 2693 (1962).

<sup>8</sup>V. Gillet, A. M. Green, and E. A. Sanderson, *Nucl. Phys.* **88**, 321 (1966).

<sup>9</sup>C. J. Batty and G. W. Greenlees, Nucl. Phys. **A133**, 673 (1969).

<sup>10</sup>M. B. Johnson, L. W. Owen, and G. R. Satchler, Phys. Rev. **142**, 748 (1966).

<sup>11</sup>J. F. Ziegler and G. A. Peterson, Phys. Rev. **165**, 1337 (1968).

<sup>12</sup>J. Saudinos, G. Vallois, O. Beer, M. Gendrot, and

L. Lopato, Phys. Letters **22**, 492 (1966).

<sup>13</sup>A. M. Bernstein, in *Advances in Nuclear Physics*, edited by M. Baranger and E. Vogt (Plenum, New York, 1969), Vol. III, pp. 325–476.

<sup>14</sup>J. Bardwick and R. S. Tickle, Phys. Rev. **161**, 1217 (1967).

PHYSICAL REVIEW C

VOLUME 5, NUMBER 2

FEBRUARY 1972

## Long-Range Fragments from Fission of $\text{U}^{236*}$

Frank H. Ruddy and John M. Alexander

*Department of Chemistry, State University of New York, Stony Brook, New York 11790*

(Received 28 September 1971)

A search for long-range fission products has been made using mica track detectors. Fission of  $\text{U}^{235}$  was induced by thermal neutrons and He gas was employed as the principal stopping material. Limits are reported for the yield of products with range greater than 20 cm He (25°C, 1 atm). The limiting yield values can be reconciled with the ternary-fission studies of Muga only if the light products from ternary fission have  $Z \geq 18$ .

Muga<sup>1, 2</sup> has reported the existence of ternary fission for several heavy nuclei. For  $\text{U}^{236*}$  produced in the thermal-neutron irradiation of  $\text{U}^{235}$ , a yield of  $\geq 1.2 \times 10^{-6}$  ternary events per binary event has been reported,<sup>1</sup> 60% of which resulted in the formation of products with a mass of approximately 25–40 amu and energy about 90 MeV.<sup>3</sup> Radiochemical<sup>4–6</sup> and mass-spectrometric<sup>7</sup> measurements have failed to pinpoint the identity of these fragments, however, and the possibilities of the formation of stable fission products or products with unique masses have been mentioned.<sup>1–3</sup>

This work is an adaptation of the technique of Natowitz *et al.*,<sup>8</sup> who studied long-range fission products from the decay of  $\text{Cf}^{252}$ . The arrangement shown in Fig. 1 was placed in a pressure-tight Lucite box which was irradiated in one of the large volume ports of the Brookhaven National Laboratory Medical Research Reactor. Two layers of mica track detectors were placed on the plastic-coated aluminum arms, marked D in Fig. 1. The target (1.23  $\mu\text{g}$   $\text{U}^{235}\text{O}_2$  plated onto 5.5  $\text{mg}/\text{cm}^2$  Ni) was placed in the well marked by a T. The well was covered with a Mylar foil (0.5  $\text{mg}/\text{cm}^2$ ) marked M. A Lexan ring marked F, which extended  $\frac{1}{8}$  in. over the target well, was used to collect fission products and thus monitor the number of fissions. The  $\gamma$  radiation from  $\text{Mo}^{99}$  and  $\text{La}^{140}$  was measured after exposure by use of a Ge(Li) detector. The irradiation resulted in about  $5 \times 10^{12}$  fissions. Mica track detectors were etched with 40% HF at 25°C for 20 min, and scanned microscopically for tracks with a pro-

jected length greater than 2.4  $\mu\text{m}$ .

The yield of tracks was measured as a function of distance from the target. Binary-fission fragments reach the end of their range at about 12–14 cm; near the end of their range they register as bright diamonds in mica.<sup>8</sup> For path lengths less than about 11.5 cm from the target, tracks from binary events were so abundant that the surface of the track detector was completely covered and scanning was impossible. The maximum detector distance from the target was 15 cm in this experiment (plus the Mylar window). Between 11.5 and 15 cm, a group of distinct tracks (not diamonds) with projected length greater than 2.4  $\mu\text{m}$  was observed. The minimum range required for a product to register such a track corresponds to the range in the Mylar window plus the range in helium plus the visible minimum range in mica. Absorber thicknesses in Mylar and mica were converted to the equivalent helium absorber thickness by using the data of Northcliffe and Schilling<sup>9</sup> for Mylar and helium, and the data of Blok *et al.*<sup>10</sup> for mica. Superficial densities were converted to equivalent distances with the following factors:

$$1 \text{ mg}/\text{cm}^2 \text{ He} = 6.1 \text{ cm He at } 1 \text{ atm } 25^\circ\text{C},$$

$$1 \mu\text{m mica} = 0.35 \text{ mg}/\text{cm}^2 \text{ mica}.$$

A plot of yield of tracks vs total range is shown in Fig. 2. The yield falls off sharply for a total range of 19 to 23 cm He. The error bars shown on the points correspond to "maximum uncertainties" in the total range.